



## Adsorption of 2,4-dichlorophenol from water using deep eutectic solvents-functionalized carbon nanotubes

Rusul Khaleel Ibrahim<sup>a,b</sup>, Mohammed Abdulhakim Al Saadi<sup>b,c,d,\*</sup>,  
Mohamed Khalid Al Omar<sup>a,b</sup>, Shaliza Ibrahim<sup>a</sup>

<sup>a</sup>Department of Civil Engineering, University of Malaya, Kuala Lumpur 50603, Malaysia,

email: rusul.alqaisy@yahoo.com (R.K. Ibrahim), mohd.alomar@yahoo.com (M.K. Al Omar), shaliza@um.edu.my (S. Ibrahim)

<sup>b</sup>University of Malaya Centre for Ionic Liquids (UMCiL), University of Malaya, Kuala Lumpur 50603, Malaysia

<sup>c</sup>Nanotechnology & Catalysis Research Centre (NANOCAT), University of Malaya, Kuala Lumpur 50603, Malaysia,

Tel. +60163630693, Fax +60 3 7967 5311, email: mdsd68j@gmail.com (M. Al Saadi)

<sup>d</sup>National Chair of Materials Sciences and Metallurgy, University of Nizwa, Sultanate of Oman, Nizwa, Oman

Received 4 November 2017; Accepted 6 May 2018

### ABSTRACT

In this work, novel adsorbents for 2,4-dichlorophenol (DCP) were introduced using deep eutectic solvent (DES) as functionalization agent for multi-wall carbon nanotubes (MWCNTs). Choline chloride salt (ChCl) was mixed with ethylene glycol (EG) as hydrogen bond donor (HBD) at molar ratio of (1:2) to prepare DES. Three DES- based MWCNTs adsorbents were produced and their chemical, physical and morphological properties were investigated using, RAMAN, FTIR, FESEM, zeta potential, TGA, TEM and BET surface area. The capability of DES as non-destructive functionalization agent for MWCNTs was proved by the increase of the purity and the surface area of MWCNTs. Response surface methodology was used to define the optimum conditions for 2,4-DCP adsorption onto each adsorbent. The adsorption experimental data were well described by pseudo-second order kinetic mode and by Langmuir isotherm model. DES-acid treated MWCNTs showed the highest maximum adsorption capacity of 390.53 mg g<sup>-1</sup>.

**Keywords:** 2,4-dichlorophenol; Deep eutectic solvents; Carbon nanotubes, Functionalization; Water treatment

### 1. Introduction

One of the most common carcinogenic chlorophenols in polluted water is 2,4-dichlorophenol (2,4-DCP), which has a pKa value of 7.4 and water solubility of 4.5 g L<sup>-1</sup> at 25°C [1]. It can be easily detected in water bodies because it is discharged from wide ranges of industries such as rubbers and plastic industries, petroleum refineries as well as herbicides and pesticides manufacture. Thus, the municipal and agricultural effluents are considered the main sources of 2,4-DCP [2–4]. The presence of 2,4-DCP in environment even at low concentrations is of a great risk due to its high

persistency, toxicity, and its organoleptic and carcinogenic effects [4–7]. As a result, 2,4-DCP is listed by Environmental Protection Agency (EPA) as one of the most hazardous contaminants that has the priority to be treated from environment [3]. Many photochemical, biochemical and electrochemical techniques have been investigated for the removal of chlorophenols from water [1,8]. Adsorption is proved to be the most effective and economic process [9] due to its ability to purify polluted water and separate pollutants from wastewater without disturbing water quality or generating toxic secondary pollutants [10–12]. Different adsorbents have been reported for 2,4-DCP removal from water, such as carbon fibers [8], multi-wall carbon nanotubes (MWCNTs) [13] and activated carbons (AC) [14–16].

\*Corresponding author.

MWCNTs have shown a great potential as competent adsorbent for the removal of various types of organic and inorganic pollutants [17–19], such as copper [20], lead [21], nickel [22], cadmium [23,24], zinc [25], phenol [26], 1,2-dichlorobenzene [27], 2,4,6-trichlorophenol [28], pentachlorophenol [29], reactive dyes [30]. Despite of the high adsorption capacity of MWCNTs for the removal of various toxic organic contaminants from water, insignificant information is reported about their adsorption capacity for the removal of 2,4-DCP [31]. Furthermore, some shortcomings hinder the application of MWCNTs including their agglomeration and their poor dispersion in aqueous solutions [32]. These shortcomings decrease the surface area of MWCNTs and reduce their ability to remove certain compounds [33]. Many studies refer to the functionalization of MWCNTs as promising attempt to overcome all the limitations restraining their application through the removal of impurities and the introduction of new different functional groups. Consequently, the solubility of MWCNTs and their graphitic networks are enhanced as well as their performance for different applications is improved [34–36]. The prevalent functionalization method can be achieved by conventional agents, either by acid treatment or by using oxidizing and reducing agents [37]. Most of these agents are considered strong and harsh solvents that usually cause unnecessary damage to the unrivaled structure of MWCNTs.

Recently, deep eutectic solvents (DESs) have been highlighted as prominent low-cost alternatives for ionic liquids (ILs) due to their high biodegradability and easy preparation process [38–40]. Generally, DES is a mixture of two or more of inexpensive and biodegradable components, namely, Salt and hydrogen bond donor (HBD). Many studies have been conducted to investigate the physiochemical properties of DESs and to involve them in different fields of biology, chemistry and electrochemistry, as well as in many nanotechnology related fields [41–43]. For example, DES of (Choline chloride: urea) was used as deposition media for the formation of gold nanoparticles (AuNPs) [44], and DES of (choline chloride: ethylene glycol) was applied as a reaction media for the production of SnO<sub>2</sub> nanocrystalline [45]. In addition, recent studies have examined the use of DESs as versatile, effective and low-cost functionalization agents to overcome the challenges restraining the application of different nanomaterials such as graphene [46] and carbon nanotubes [47–49]. The advantage of DES as functionalization agent was confirmed by improving the dispersion of nanomaterials through attaching new valuable functional groups to their surface, and unlike conventional functionalization agents, DES causes no damage to the structure of nanomaterials and conserve their exquisite electrical and mechanical properties.

In this study, choline chloride (ChCl) and ethylene glycol (EG) were used to synthesize [ChCl:EG] DES which was used as novel functionalization agent for MWCNTs. Then, the chemical, physical and morphological changes on MWCNTs after treatment with DES were comprehensively studied using different analytical techniques including RAMAN, FTIR, BET surface area, TEM, FESEM, TGA and zeta potential. Subsequently, DES-MWCNTs combinations were used for the first time as new adsorbents for 2,4-DCP in aqueous solution. Optimization, kinetics and isotherms studies were carried out to describe the optimum adsorp-

tion conditions and to illustrate the adsorption mechanism of 2,4-DCP on DES-functionalized MWCNTs.

## 2. Experimental

### 2.1. Materials

MWCNTs with specifications of D × L 6–9 nm × 5 μm N > 95% (carbon) was supplied by sigma Aldrich and DCP with a molecular weight of 163.0 g·mol<sup>-1</sup> was used as adsorbate and supplied by Merck. Other chemicals including, sulfuric acid H<sub>2</sub>SO<sub>4</sub> (95%–97%), sodium hydroxide pellets NaOH, Choline chloride ChCl (≥ 98 %), potassium permanganate KMnO<sub>4</sub>, hydrochloric acid HCL (36.5%–38%) were supplied by sigma Aldrich, while ethylene glycol EG (≥ 98%), acetonitrile ACN and methanol MeOH, were supplied by Merck.

### 2.2. DES preparation

The used DES [ChCl:EG] was produced by combining ChCl (salt) with EG (HBD) at [1:2] molar ratio. The salt and HBD were mixed at 180 rpm and a temperature of 70°C for a period of 80 min until a homogeneous transparent liquid formed. The prepared DES was stored in a moisture-controlled environment for further functionalization use.

### 2.3. Functionalization of MWCNTs

#### 2.3.1. Acidification and oxidation

Primarily, pristine MWCNTs (P-MWCNTs) were dried overnight at 100°C. Half of the dried MWCNTs amount was refluxed with 50% H<sub>2</sub>SO<sub>4</sub> for 1 h at 140°C to prepare S-MWCNTs and the other half was sonicated with KMnO<sub>4</sub> for 2 h at 60°C to prepare K-MWCNTs. Both S-MWCNTs and K-MWCNTs were then washed using vacuum filtration system until the pH value of the washing water became neutral and they were dried under vacuum for 24 h at 100°C.

#### 2.3.2. Functionalization with DES

A specific amount of 200 mg of each acidified and oxidized MWCNTs were sonicated separately with 7 ml of DES for 3 h at 60°C to produce DES-P-MWCNTs, DES-S-MWCNTs and DES-K-MWCNTs (see Table 1). Then the produced adsorbents were washed using vacuum filtration system and dried under vacuum for 24 h at 100°C.

Table 1  
Abbreviation and modification method of examined adsorbents

Adsorbent abbreviation	Modification method
P-MWCNTs	Pristine
S-MWCNTs	Acidification with sulfuric acid
DES-P-MWCNTs	Sonication with [ChCl:EG]
DES-S-MWCNTs	Acidification + Sonication with [ChCl:EG]

#### 2.4. Batch adsorption studies

The concentration of 2,4-DCP was determined using ultra high-performance chromatography (Waters ACQUITY UPLC System) at wavenumber of 285 nm (60 ACN: 40 MeOH). A primary adsorption screening was conducted to compare the removal efficiency of all produced adsorbents. A fixed dosage of each adsorbent (10 mg) was shaken at room temperature into 50 ml of a 2, 4-DCP stock solution of 10 mg L<sup>-1</sup> at a constant agitation speed of 180 rpm. Design expert (DE) software (version 7.0) was used to optimize the conditions of 2,4-DCP removal. The response surface was set as a type of study and the central composite design (CCD) was adopted to conduct the adsorption experiment. The optimization study was determined by setting one responding parameter (i.e. removal %) and by setting a range of three different parameters including, pH (2–10), dose (5–15 mg), and contact time (20–60 min). List of design of experiments runs and actual values obtained from each response are provided in the supporting information (Table S1).

The adsorption kinetics experiment was performed by using the optimum conditions of each adsorbent suggested by DE software. The contact times used to define the suitable kinetic model were (5 min, 10 min, 20 min, 30 min, 60 min, 120 min, 180 min and 24 h). Pseudo first order, pseudo second order models were applied on the experimental data. Furthermore, various initial concentrations were used to conduct the adsorption isothermal experiments (5, 10, 20, 30, 40, 50, 60 and 80 mg L<sup>-1</sup>). The isotherm study examined the suitability of four isotherm models (e.g. Langmuir and Freundlich, Temkin, and Dubinin-Radushkevich isotherm models).

#### 2.5. Characterization

Fourier transform infrared (FTIR) spectroscopy Perkin-Elmer® FTIR spectrometer was used to study the functional groups of MWCNTs after and before the functionalization process. Raman shift for all adsorbents was obtained by Raman spectroscopy (Renishaw System 2000 Raman Spectrometer). The surface charge was evaluated by the zeta potential using Zetasizer (Malvern, UK). The thermal stability of all adsorbents was analyzed using thermogravimetric analysis (TGA) and differential thermogravimetry (DTG) by Thermal Analyzer (STA-6000, PerkinElmer®). Field Emission Scanning Electron Microscope (JEOL Ltd., Japan. JSM-6700F) was used to obtain high resolution images to observe the morphology of all concerned adsorbents. The effect of functionalization with DES was investigated using Transmission Electron Microscopy (TEM). Finally, the surface area for all examined adsorbents was estimated using a fully Automated Gas Sorption System (micromeritics, TriStar II 3020, USA) based on the method of Brunauer-Emmett-Teller (BET).

### 3. Results and discussion

#### 3.1. Primary screening

The result of the primary screening is visualized by Fig. 1. It is remarkable that P-MWCNTs, S-MWCNTs, DES-P-MWCNTs and DES-S-MWCNTs achieved removal efficiencies higher than that of K-MWCNTs and DES-K-MWCNTs

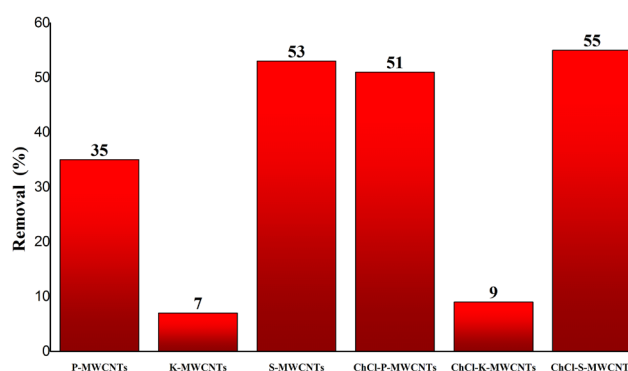


Fig. 1. Screening of adsorbents for the removal of 2,4-DCP

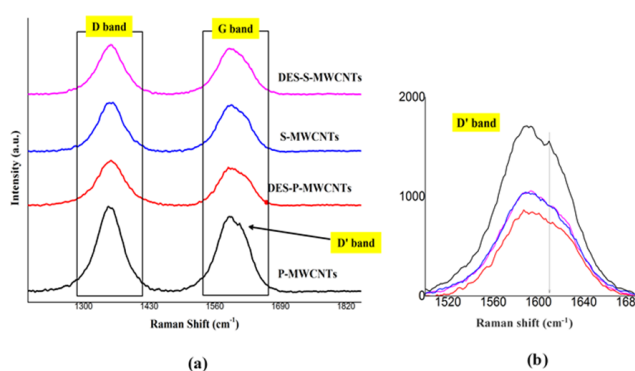


Fig. 2. Raman spectroscopy of P-MWCNTs, S-MWCNTs, DES-P-MWCNTs and DES-S-MWCNTs for a) D band and G band, and b) D' band shift.

and this can be ascribed to the surface charge of the adsorbents. Therefore, this study will focus on characterization and investigation of the adsorption performance of only adsorbents with the highest removal (%).

#### 3.2. Characterizations

##### 3.2.1. Raman spectroscopy

As can be noticed from Fig. 2 all concerned adsorbents show two obvious sharp peaks detected at ~1350 and ~1590 cm<sup>-1</sup> wavelength. The peak at 1300–1400 cm<sup>-1</sup> is the D band which is a defect-induced mode caused by sp<sup>3</sup>-hybridized carbon atoms in the sidewall of CNT and it is often attributed to the existence of amorphous and disordered carbon in the CNT samples [36,50–52]. While peak at 1550–1680 cm<sup>-1</sup> is the G band which is a common tangential mode to all sp<sup>2</sup> carbon systems and it is raised from the stretching of C–C bond in graphitic materials [53]. Moreover, D' is also a defect or disorder induced Raman feature presented by a weak shoulder of the G-band, can be clearly found in P-MWCNTs and DES-P-MWCNTs at 1609 cm<sup>-1</sup> and 1612 cm<sup>-1</sup> wavelength, respectively. Whereas for S-MWCNTs and DES-S-MWCNTs, D' cannot be detected which indicates a better quality of these two adsorbents [54]. Another Raman feature is the radial breathing mode (RBM) which is considered an important feature to identify the tube diameter [53]. However, RBM was too weak to be detected for all studied adsorbents which proves the large diameter of their tubes [36].

Table 2  
Raman spectroscopy bands intensities and locations

Adsorbent	D band		G band		D' band		$I_D/I_G$
	Wave No.	Intensity	Wave No.	Intensity	Wave No.	Intensity	
P-MWCNTs	1349	1942	1589	1710	1609	1558	1.11
S-MWCNTs	1358	1114	1592	1056	–	–	1.05
DES-P-MWCNTs	1353	1023	1594	846	1612	741	1.2
DES-S-MWCNTs	1353	1131	1588	1044	–	–	1.08

Furthermore, Raman spectroscopy can be a symptomatic characterization of the degree of carbon-containing defects by calculating the ratio of D band intensity to G band intensity ( $I_D/I_G$ ) [55]. The values of  $I_D/I_G$  for all adsorbents are listed in Table 2. It is evident from Table 2 that  $I_D/I_G$  for P-MWCNTs has increased from 1.11 to 1.20 after treatment with DES and that gives an indication of new sp<sup>3</sup>-hybridized functional groups formation on the P-MWCNTs surface [47]. It is also apparent from Table 2 that the value of  $I_D/I_G$  of P-MWCNTs has decreased after H<sub>2</sub>SO<sub>4</sub> treatment which suggests that S-MWCNTs adsorbent has less carbon-containing defects and more graphitized structures [56]. However,  $I_D/I_G$  ratio for S-MWCNTs has increased slightly after treatment with DES which could be due to the increased level of covalent functionalization on the surface of DES-S-MWCNTs.

### 3.2.2. FTIR

Fig. 3 displays the FTIR spectra for all adsorbents. Obviously, there is a significant change in the spectrum of P-MWCNTs after treatment with acid and DES and that confirms the capability of the functionalization process by the addition of new and abundant functional groups onto the surface of P-MWCNTs. The strong absorbance peak at ~3460 cm<sup>-1</sup> for all functionalized MWCNTs is assigned to O–H stretching bond (hydroxyl groups) [57]. However, O–H may overlap with N–H stretching bond in the region of (3500–3000) cm<sup>-1</sup> [58]. The emergence of peaks at ~3750 cm<sup>-1</sup> after functionalization are assigned to C–H stretching bond. Furthermore, asymmetric and symmetric stretching of CH<sub>2</sub> groups are highly detectable at ~2900 cm<sup>-1</sup> and ~2800 cm<sup>-1</sup>, respectively [59]. All adsorbents showed an obvious peak around 2350 cm<sup>-1</sup> which is assigned to aromatic sp<sup>2</sup> C–H stretching vibration [60]. Moreover, the production of carbonyl groups and carboxylic acids onto P-MWCNTs after functionalization is symbolized by the presence of peaks at ~1400 and ~1650 cm<sup>-1</sup> [61]. Functionalization of P-MWCNTs with H<sub>2</sub>SO<sub>4</sub> produced different bonds involving sulfur such as C–S stretching (700–600) cm<sup>-1</sup> and SO<sub>2</sub> symmetric stretching (1153) cm<sup>-1</sup> [62]. Peaks in the region between (800–600) cm<sup>-1</sup> are assigned to C–Cl bond for all DES treated adsorbents [49]. Table 3 summarizes some of expected functional groups onto the studied adsorbents.

### 3.2.3. TGA

The oxidation behavior of all adsorbents was investigated using thermal gravimetric analysis under air flow

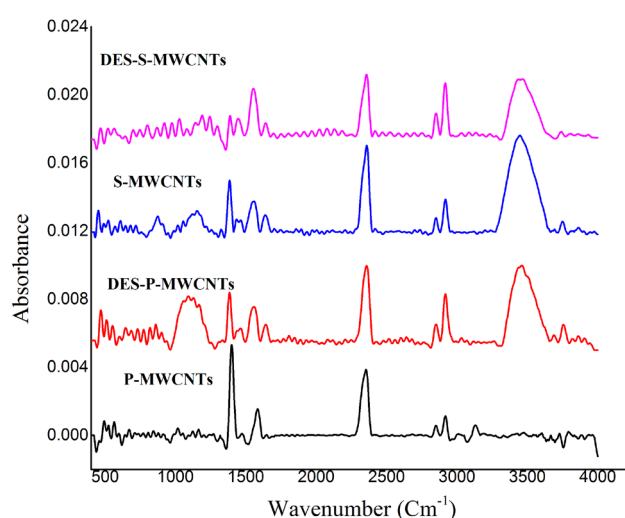


Fig. 3. FTIR spectrum for P-MWCNTs, S-MWCNTs, DES-P-MWCNTs, and DES-S-MWCNTs.

rate of 50 mL/min at a temperature range of 25–800°C with a heating rate of 10°C/min. Fig. 4 reveals that all adsorbents have high thermal stability and show a weight loss of 3.8–8% below 500°C. It can be noticed from Fig. 4 that a significant combustion of P-MWCNTs starts at 526.6°C, while the noteworthy combustion of S-MWCNTs, DES-P-MWCNTs and DES-S-MWCNTs start 530.28°C, 510.06°C and 516.9°C, respectively. It is widely known that the amorphous carbons tend to oxidize at temperature lower than that required for the oxidation of well graphitized structure [20] [63–65]. Accordingly, S-MWCNTs adsorbent has a higher purity among all examined adsorbents and that agrees with the results obtained from Raman analysis. Furthermore, it is obvious that functionalization with DES caused a slight reduction in the onset of adsorbent combustion due to the presence of various kinds of functional groups that have a lower activation energy for oxidation (see FTIR section). The weight loss for all functionalized adsorbents was very little at temperature > 590°C and it reached 0% at around 606.05°C with no residues left, while at the same temperature the remaining weight of P-MWCNTs was 30.09%. Based on that, treatment of P-MWCNTs with acid and/or DESs effectively increased the purity and the carbon content of P-MWCNTs.

Table 3  
Some of the predicted functional groups on the surface of the studied adsorbents

Expected functional groups	Involving adsorbents
C–H stretching	ALL
C=O	ALL
C=C–C Aromatic ring stretch	ALL
S–S stretching	DES-S-MWCNTs, S-MWCNTs.
C–S stretching	DES-S-MWCNTs, S-MWCNTs.
SO <sub>2</sub> symmetric and asymmetric stretching	DES-S-MWCNTs, S-MWCNTs.
S=O stretching	DES-S-MWCNTs.
O–CH <sub>3</sub>	DES-P-MWCNTs, S-MWCNTs, DES-S-MWCNTs.
C–Cl	DES-P-MWCNTs, DES-S-MWCNTs.
N–H stretching Third overtone	DES-P-MWCNTs, DES-S-MWCNTs.

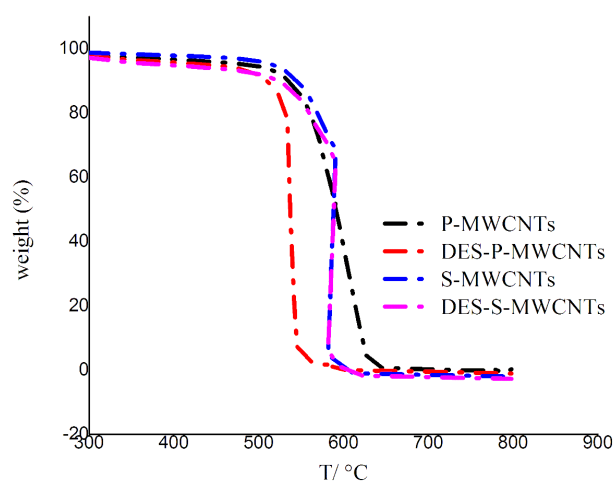


Fig. 4. TGA curves for P-MWCNTs, S-MWCNTs, DES-P-MWCNTs, and DES-S-MWCNTs.

### 3.2.4. Zeta potential

Zeta potential was measured by discrete dispersion of 2.5 mg of each adsorbent in 5 mL of deionized water. The order of the results is presented in Fig. 5. It is clear that S-MWCNTs, DES-P-MWCNTs and DES-S-MWCNTs have more negative surface charges than P-MWCNTs due to the presence of more oxygen-containing groups such as carbonyl, carboxyl and hydroxyl groups as revealed in FTIR analysis [66,67]. The significant variation in the absolute value of zeta potential for P-MWCNTs after functionalization is related to the influence of hydrophilicity or hydrophobicity properties of various kinds of functional groups formed on the surface of functionalized MWCNTs. The treatment of P-MWCNTs either with acid or DES increased the zeta potential absolute value which indicates a better stability and assures the increase in the functionality degree of the functionalized MWCNTs [68].

### 3.2.5. BET surface area

The surface area for P-MWCNTs, S-MWCNTs, DES-P-MWCNTs and DES-S-MWCNTs was evaluated using BET



Fig. 5. Arrangements of zeta potential values for P-MWCNTs, S-MWCNTs, DES-P-MWCNTs, and DES-S-MWCNTs.

method. Table 4 shows the surface area, pore volume and diameter for all adsorbents. It is noticeable that the surface area of P-MWCNTs has interestingly increased after functionalization with acid or/and DES. This significant increase in the surface area of functionalized MWCNTs can be attributed to the removal of impurities on P-MWCNTs-surface by H<sub>2</sub>SO<sub>4</sub> or by DES and that was corroborated by TGA results. Thus, the maximum adsorption capacity for the functionalized MWCNTs is much higher than that of P-MWCNTs.

### 3.2.6. TEM, FESEM

Fig. 6 and Fig. S1 (supporting information) represent the TEM and FESEM images for pristine and functionalized MWCNTs. It is obvious that there is no significant destruction in the structure of MWCNTs, which proposes that the functionalization with DES is a non-destructive functionalization and it ensures the unique properties of MWCNTs and enhances the interfacial properties between the adsorbents and the pollutants. Furthermore, after acid treatment, more agglomeration-like behavior is observed and DES has a significant cleaning effect by removing the agglomeration produced by acid.

## 3.3. Response surface methodology (RSM)

### 3.3.1. Analysis of variance (ANOVA)

The reduced cubic model analysis (ANOVA) of removal (%) response for P-MWCNTs and for S-MWCNTs is listed in Table S2, whereas reduced cubic model (ANOVA) of removal (%) for DES-P-MWCNTs and DES-

Table 4  
BET surface area, pore volume and diameter of all adsorbents

Property	P-MWCNTs	S-MWCNTs	DES-P-MWCNTs	DES-S-MWCNTs
BET surface area (m <sup>2</sup> /g)	123.54	226.11	197.8	193.10
Total pore volume (cm <sup>3</sup> /g)	0.62	1.45	1.19	1.22
Average pore diameter (Å)	20.49	256.84	241.28	254.21

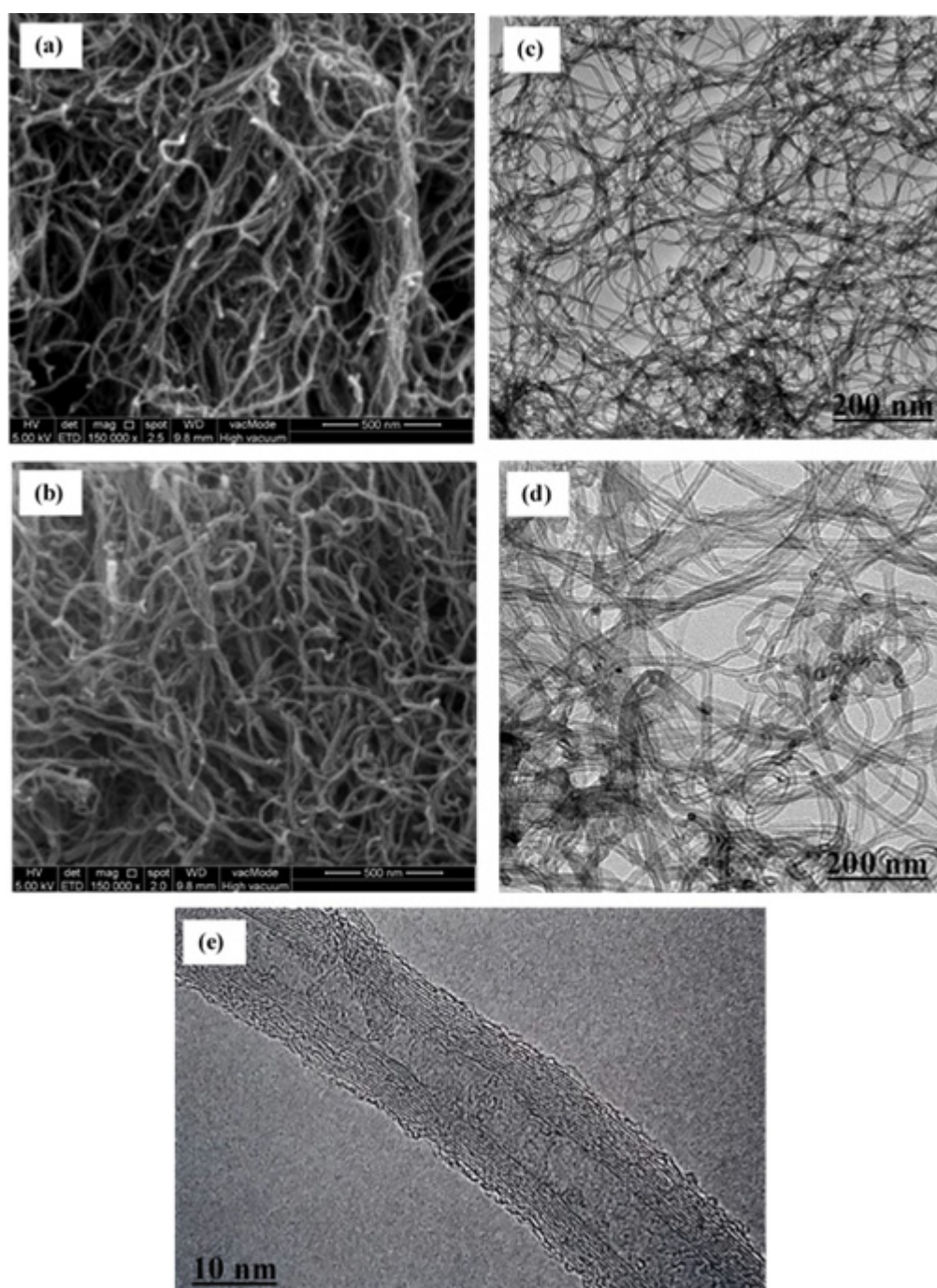


Fig. 6. FESEM images for a) P-MWCNTs, b) DES-S-MWCNTs; and TEM images for c) P-MWCNTs, d) and e) DES-S-MWCNTs.

Table 5  
Reduced cubic model analysis of variance (ANOVA) for 2,4-DCP removal (%) by DES-P-MWCNTs and DES-S-MWCNTs

Source*	DES-P-MWCNTs					DES-S-MWCNTs				
	Sum of squares	df	Mean square	F-value	p-value prob> F	Sum of squares	df	Mean square	F-value	p-value prob> F
Model	10503.64	9	1167.07	26.38	0.0105	7375.88	9	819.54	37.76	0.0062
A	5343.95	1	5343.95	120.79	0.0016	2834.06	1	2834.06	130.59	0.0014
B	485.38	1	485.38	10.97	0.0453	46.28	1	46.28	2.13	0.2403
C	1.40	1	1.40	0.032	0.8701	14.71	1	14.71	0.68	0.4706
AB	783.79	1	783.79	17.72	0.0245	397.44	1	397.44	18.31	0.0234
AC	69.06	1	69.06	1.56	0.3001	32.04	1	32.04	1.48	0.3112
BC	32.94	1	32.94	0.74	0.4517	108.77	1	108.77	5.01	0.1111
A <sup>2</sup>	748.44	1	748.44	16.92	0.0260	1009.14	1	1009.14	46.50	0.0065
B <sup>2</sup>	51.76	1	51.76	1.17	0.3586	2.84	1	2.84	0.13	0.7417
C <sup>2</sup>	259.21	1	259.21	5.86	0.0941	453.44	1	453.44	20.89	0.0196
	<b>Adj R-Squared**</b>		<b>0.95</b>	<b>Pred R-Squared</b>	<b>0.77</b>	<b>Adj R-Squared**</b>		<b>0.96</b>	<b>Pred R-Squared</b>	<b>0.76</b>
	<b>C.V. %</b>		<b>18.78</b>	<b>Std. Dev</b>	<b>6.65</b>	<b>C.V. %</b>		<b>11.58</b>	<b>Std. Dev</b>	<b>4.66</b>

\*A: pH, B: adsorbent dosage and C: contact time; \*\* The “Pred R-Squared” is in reasonable agreement with the “Adj R-Squared”

S-MCNTs is listed in Table 5. The model F-values for all adsorbents confirmed that all models are statistically significant. There is only a 1.05%, 0.62%, chance that the Model F-value can occur due to noise for the removal (%) response of DES-P-MWCNTs and DES-S-MWCNTs, respectively. The desirable value of signal to noise ratio should be greater than 4 and it is represented by the Adeq Precision value. Based on that, for all adsorbents, the models showed a ratio value greater than 4 which indicates an adequate signal.

The relationship between the independent variables and the removal % (R %) for all adsorbents is expressed by the following quadratic equations:

$$2,4\text{-DCP R \% of P-MWCNTs} = 72.17 - 26.24A + 10.29B + 20C - 11.34AB - 2.47AC - 2.17BC - 29.21A^2 - 4.27B^2 - 10.11C^2 \quad (1)$$

$$2,4\text{-DCP R \% of S-MWCNTs} = 71.88 - 29.15A + 6.05B + 1.28C - 7.37AB + 1.14AC - 1.96BC - 29.95A^2 - 5.19B^2 - 11.33C^2 \quad (2)$$

$$2,4\text{-DCP R \% of DES-P-MWCNTs} = 66.23 - 25.61A + 7.72B - 0.37C - 9.90AB - 2.94AC - 2.03BC - 22.96A^2 - 6.04B^2 - 12.38C^2 \quad (3)$$

$$2,4\text{-DCP R \% of DES-S-MWCNTs} = 73.50 - 18.65A + 2.38B - 1.21C - 7.05AB + 2.00AC - 3.69BC - 26.66A^2 - 1.41B^2 - 16.37C^2 \quad (4)$$

where A, B, C represent pH, Dosage (mg) and contact time (min), respectively. The predicted values of removal % calculated from ANOVA model equations along with the actual values for all adsorbents are listed in Table S3. The predicted values were plotted versus the experimental data for all examined adsorbents (Fig. 7). It can be observed that the experimental data are in close agreement with the

data predicted by the suggested models which proves that all models have significantly generated a good correlation between the variables of the process. The correlation coefficient R<sup>2</sup> value for removal % response for all studied adsorbents is greater than 0.98 and that confirms the competence of the models adopted for the studied adsorbents.

### 3.3.2. The interactive effects of selected independent parameters on the adsorption of 2,4-DCP

The removal (%) of all used adsorbents over different combination of independent variables were presented by three-dimension view of response surface plot as a function of two independent parameters (Figs. 8 and 9). The initial concentration of 2,4-DCP was constant for all cases with a value of 10 mg L<sup>-1</sup>. It is obvious that for all adsorbents, the removal (%) increases gradually with the increase of contact time until the system reached equilibrium. Table 6 shows some constraints and different levels of importance which were set for optimization of four goals (i.e. contact time, pH, adsorbent dosage, and removal (%) of 2,4-DCP) to select the optimum conditions for 2,4-DCP adsorption onto the studied adsorbents. The effect of pH value is noticeable on the removal (%) as it affects the properties of both adsorbate and adsorbents. Adsorption of 2,4-DCP clearly decreases as the pH value increases. This can be explained by the deprotonation of some functional groups onto the surface of the adsorbent resulting in more negatively charged surface [69]. As well as, high pH value leads to more dissociation of 2,4-DCP molecules into C<sub>6</sub>H<sub>3</sub>Cl<sub>2</sub>O<sup>-</sup> form, subsequently increasing the electrostatic repulsion and reducing the adsorption capacity [70]. Moreover, 2,4-DCP adsorption is enhanced with the decrease of pH value and the removal (%) reached to its maximum value at pH 3.87 and 5.14 for DES-P-MWCNTs and DES-S-MWCNTs, respectively (Table S4). This can be attributed to the presence of 2,4-DCP in non-dissociated form and the surface of the adsorbent is highly protonated at acidic pH value, leading to an easy

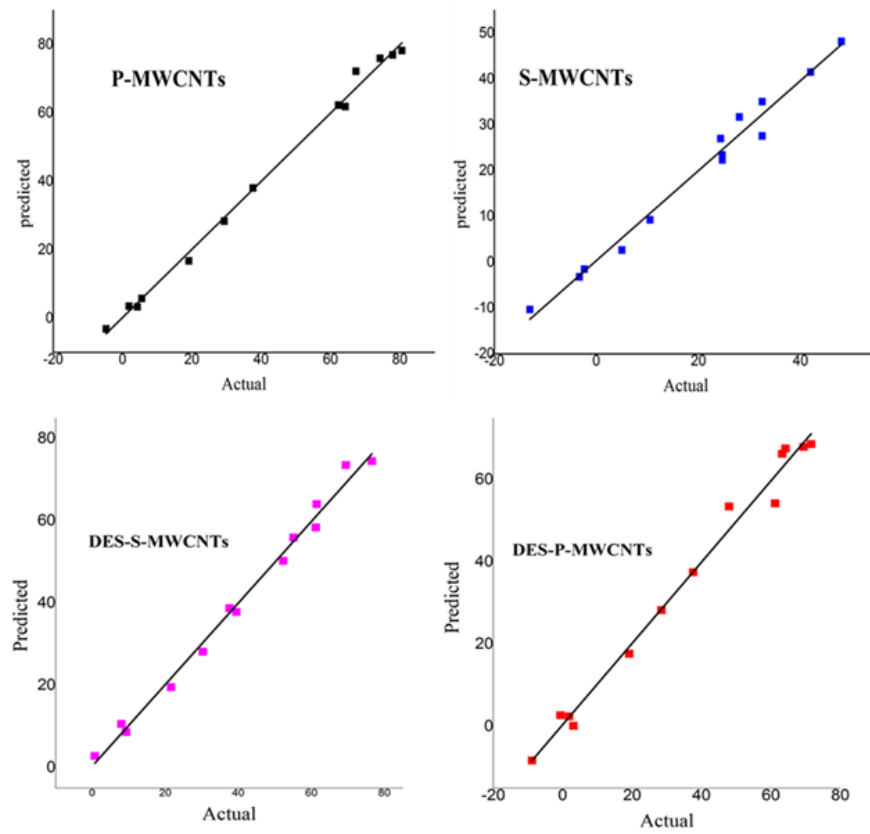


Fig. 7. Predicted values vs actual values for 2,4-DCP removal response.

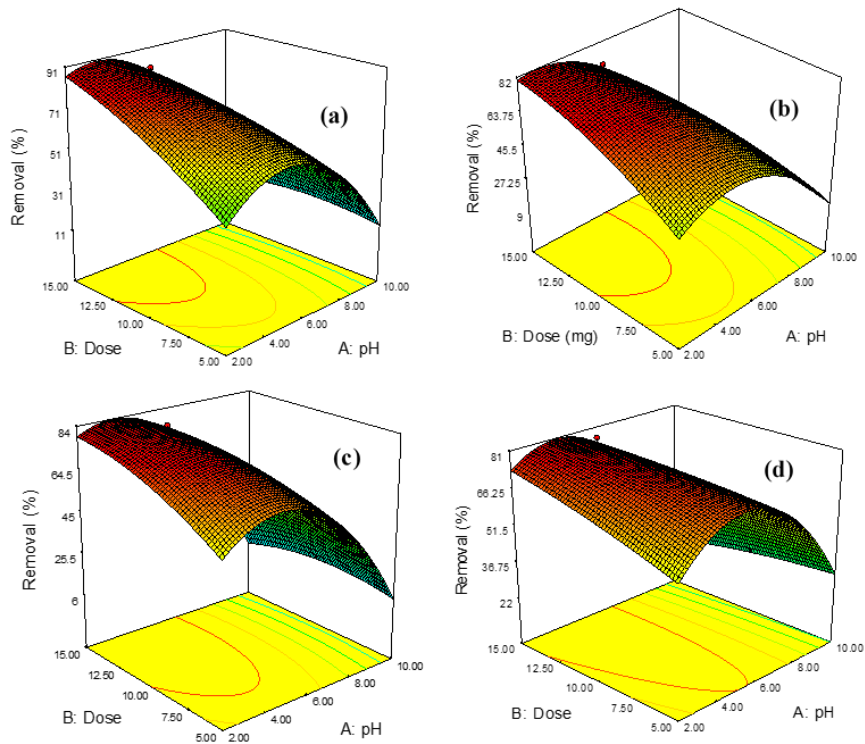


Fig. 8. Surface response representation of removal (%) of 2,4-DCP interaction with adsorbent dose and pH by fixing contact time at the optimum value for: (a) P-MWCNTs, (b) DES-P-MWCNTs, (c) S-MWCNTs, and (d) DES-S-MWCNTs.

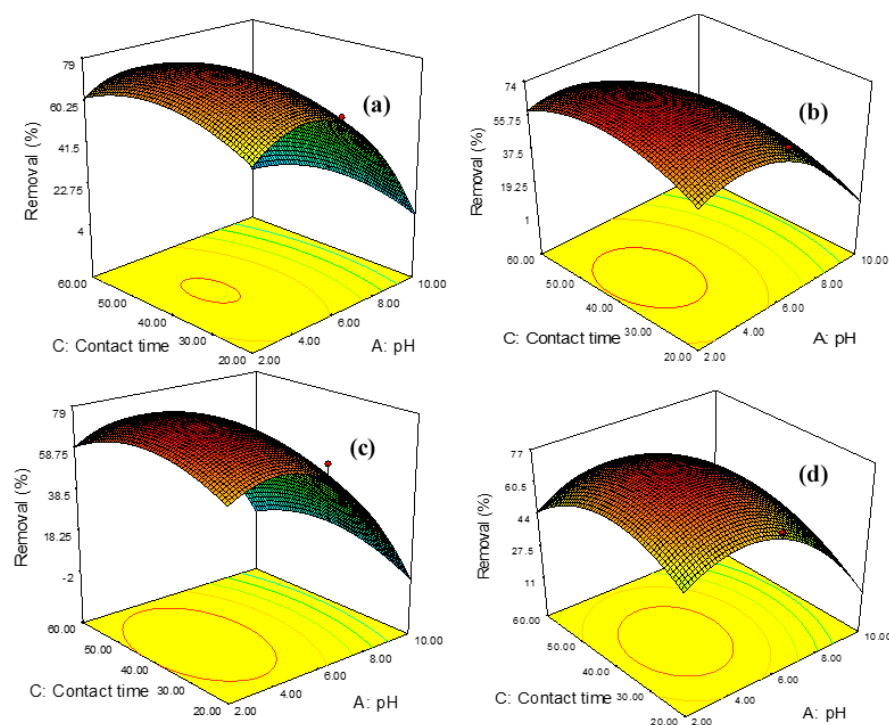


Fig. 9. Surface response representation of removal (%) of 2,4-DCP interaction with contact time and pH by fixing adsorbent dosage at the optimum value for: (a) P-MWCNTs, (b) DES-P-MWCNTs, (c) S-MWCNTs, and (d) DES-S-MWCNTs.

Table 6  
Constraints for optimization process based on CCD for 2,4-DCP adsorption

Name	Goal	Lower limit	Upper limit	Importance
A	In range	2	10	–
B	Minimize	5	15	1
C	In range	20	60	–
R% P-CNTs	Maximize	1.8	80.6	5
PChCl-CNTs		1.85	71.5	
S-CNTs		3.7	75.5	
SChCl-CNTs		0.68	76.53	

A: pH, B: adsorbent dosage and C: contact time

adsorption process by high electrostatic attraction between the adsorbent and the adsorbate [71]. Meanwhile, the dose of the adsorbent has an obvious effect on 2,4-DCP removal efficiency. Fig. 8 reveals that the removal (%) increases along with the increase of the adsorbent dose and that can be ascribed to the increase of surface area and the availability of more adsorptive sites for the removal of 2,4-DCP.

### 3.4. Adsorption kinetics and isotherms

#### 3.4.1. Kinetics study

Two kinetic models, pseudo-first-order kinetic model and pseudo-second-order kinetic model, were applied to the experimental data. The linear form of the pseu-

do-first-order model proposed by Lagergren and Svenska [Eq. (5)] [72–74]:

$$\ln(q_e - q_t) = \ln q_e - k_1 t \quad (5)$$

where  $q_e$  and  $q_t$  ( $\text{mg g}^{-1}$ ) are the amounts of the adsorbed 2,4-DCP at equilibrium and at time  $t$  (min), respectively, and  $k_1$  is the adsorption rate constant ( $\text{min}^{-1}$ ). The values of  $q_e$  and  $k_1$  were obtained from the intercept and slope respectively of plots of  $\ln(q_e - q_t)$  vs.  $t$  (Fig. 10a) and they are listed in Table 7.

The linearized form of pseudo-second-order kinetic model is expressed as below [75,76]:

$$\frac{t}{q_t} = \frac{1}{k_2 q_e^2} + \frac{t}{q_e} \quad (6)$$

where  $k_2$  ( $\text{g mg}^{-1} \text{min}^{-1}$ ) is the rate constant of the second order adsorption. The values of  $k_2$  and  $q_e$  were determined from the slope and intercept of plots of  $t/q_t$  vs.  $t$  (Fig. 10b) and they are listed in Table 7.

It is obvious from Table 7 that the calculated values of Pseudo-first-order kinetic does not agree with the experimental values, while for Pseudo-second-order kinetic the calculated values of agree with the experimental values. Not to mention, for all examined adsorbents the correlation coefficient ( $R^2$ ) value of Pseudo-second-order model is 0.99 which is much higher than that of Pseudo-first-order model (0.69–0.80). Therefore, the adsorption of 2,4-DCP on pristine/functionalized MWCNTs is not a first order reaction and it is ideally obeying the Pseudo-second-order kinetic model. These findings are in agreement with some reported kinetics results for 2,4-DCP adsorption on carbonaceous adsorbents

Table 7  
Adsorption kinetics constants and correlation coefficient for each model

Adsorbent	$q_e$ (experimental)	Pseudo-first order			Pseudo-second order		
		$R^2$	$K_1$	$q_e$	$R^2$	$K_2$	$q_e$
P-MWCNTs	37.5	0.69	0.01	9.34	0.99	0.0065	38.01
S-MWCNTs	38.82	0.80	0.01	13.23	0.99	0.0041	39.57
DES-P-MWCNTs	40.22	0.69	0.01	16.13	0.99	0.0023	41.92
DES-S-MWCNTs	60	0.79	0.01	22.96	0.99	0.002	61.69

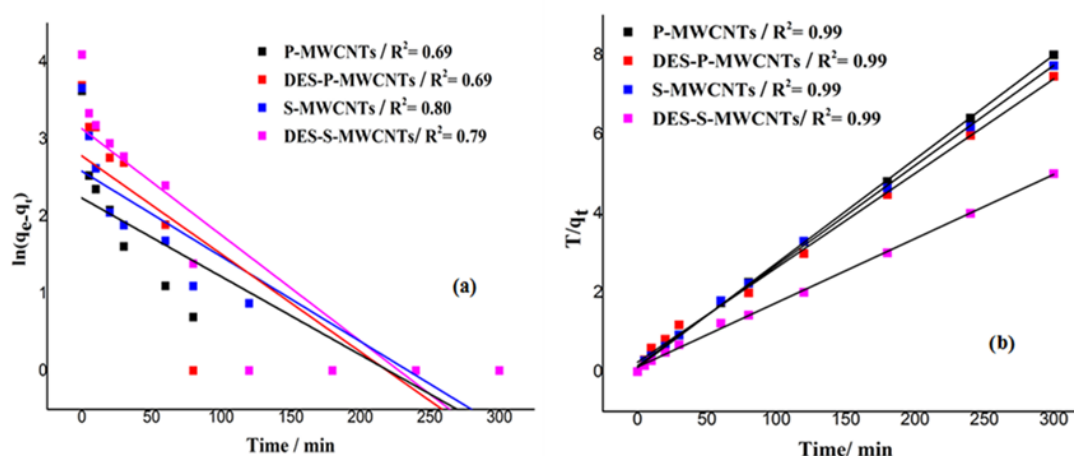


Fig. 10. Kinetic models for 2,4-DCP adsorption: (a) Pseudo-first-order kinetic model and (b) Pseudo-second-order kinetic model.

[69] and on activated carbon fiber [8]. Similar kinetic results were reported for the adsorption of 2,4-DCP onto activated carbon fiber [77] and onto Mn-modified activated carbon prepared from Polygonum Orientale Linn [78]. The applicability of Pseudo-second-order kinetic model to describe the adsorption of 2,4-DCP in this study indicates that the adsorption process rate is controlled by chemisorption involving valence forces through exchange or sharing electrons which suggests the possibility of adsorbate and adsorbent involvement in the adsorption mechanism [79–81].

### 3.4.2. Isotherms study

The well-known linearized form of Langmuir equation is presented in Table 8. In the equation,  $C_e$  ( $\text{mg L}^{-1}$ ) is the equilibrium concentration of 2,4-DCP,  $q_e$  ( $\text{mg g}^{-1}$ ) is the amount of 2,4-DCP adsorbed per unit mass of the adsorbent.  $K_L$  and  $Q_m$  are Langmuir constants related to adsorption equilibrium constant and maximum adsorption capacity, respectively. The value of the dimensionless constant equilibrium parameter ( $R_L$ ) can be used to indicate the essential feature and the type of Langmuir isotherm: unfavorable ( $R_L > 1$ ), linear ( $R_L = 1$ ), favorable ( $0 < R_L < 1$ ) or irreversible ( $R_L = 0$ ) [82,83]. The following equation (Eq. (7)) is used to calculate  $R_L$  value [84]:

$$R_L = \frac{1}{1 + K_L C_e} \quad (7)$$

Freundlich isotherm can be described by the linearized equation shown in Table 8. where,  $K_f$  and  $n$  are Freundlich

isotherm constants, and the distribution coefficient  $K_f$  represents the amount of 2,4-DCP adsorbed onto the tested adsorbents for a unit equilibrium concentration [85]. The heterogeneity factor  $1/n$  defines the heterogeneity of the adsorbent surface and as its value is getting closer to zero the adsorbent surface is becoming more heterogeneous [85,86].

Moreover, the Temkin and Dubinin-Radushkevich (DRK) isotherm models were examined for their suitability to describe the experimental results and their linear equations are listed in Table 8. The parameters of Temkin equations are: which is the Temkin isotherm equilibrium binding constant ( $L \text{ mg}^{-1}$ ) and  $B$  (dimensionless) =  $RT/b$  (where  $b$  is the Temkin constant related to the heat of adsorption ( $\text{J mol}^{-1}$ ),  $R$  is the gas constant ( $8.314 \text{ J mol}^{-1} \text{ K}^{-1}$ ),  $T$  is the absolute temperature in kelvin, i.e. room temperature =  $298.15 \text{ K}$ ). On the other hand, the parameters of DRK isotherm include  $E$  which is the mean free adsorption energy ( $\text{J mol}^{-1}$ ),  $Q_s$  is the theoretical isotherm saturation capacity ( $\text{mg g}^{-1}$ ),  $K$  is the constant of DRK isotherm, and  $\epsilon$  represents the Polanyi potential and can be expressed as:

$$\epsilon = RT \ln(1 + 1/C_e) \quad (8)$$

Langmuir, Freundlich and Temkin isothermal plots of all adsorbents are shown in Fig. 11 as well as the constants and all correlation factors of all models are summarized in Table 8. As can be observed, the values of  $R_L$  and  $n$  for all concerned adsorbents confirm the adsorption favorability of 2,4-DCP for both Langmuir and Freundlich adsorption

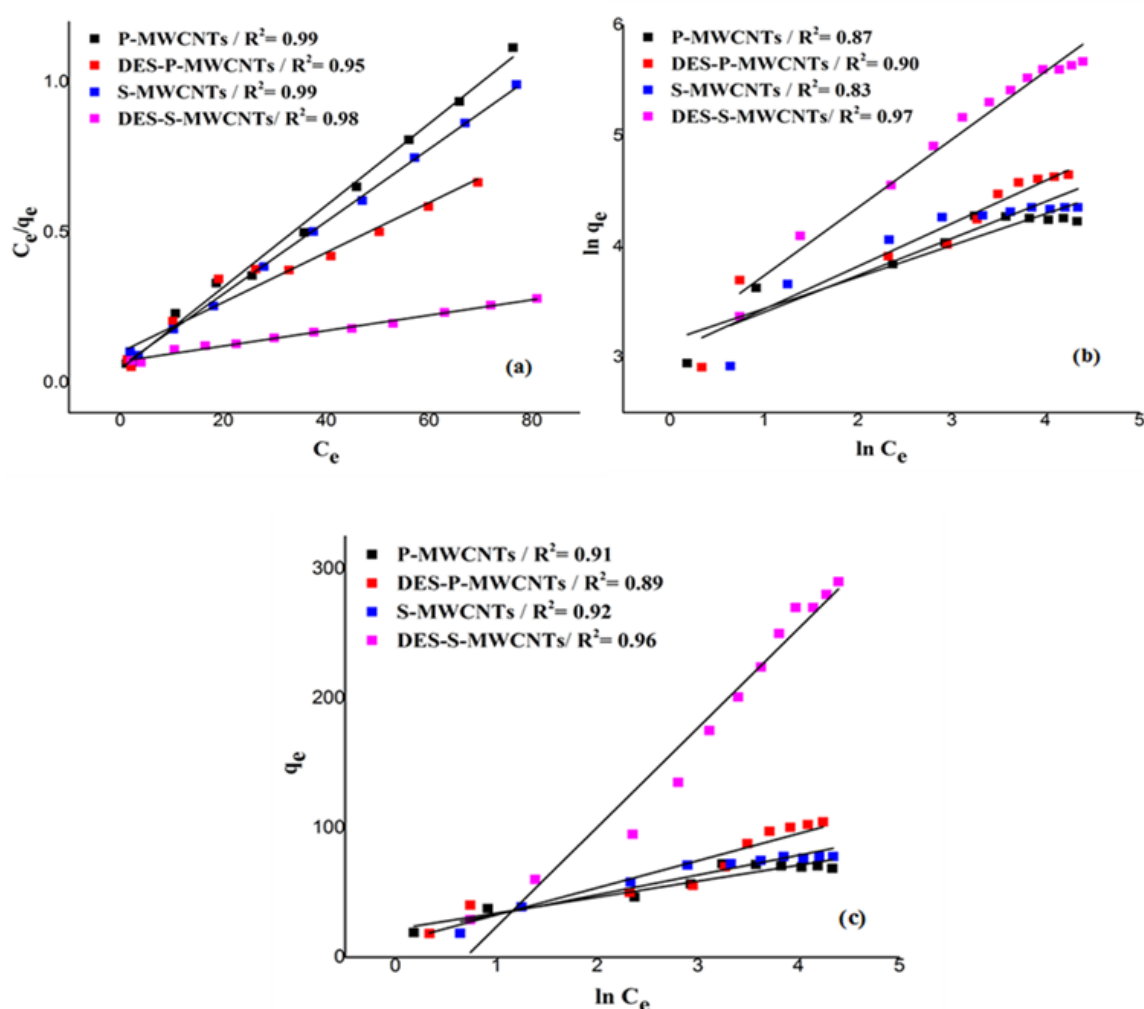


Fig. 11. Isotherm models for 2,4-DCP adsorption: (a) Langmuir isotherm, (b) Freundlich isotherm and (c) Temkin isotherm models.

Table 8  
Equations, constants and correlation coefficients of isotherm models

Isotherms	Equations	Parameters	Adsorbents			
			P-MWCNTs	S-MWCNTs	DES-P-MWCNTs	DES-S-MWCNTs
Langmuir	$\frac{C_e}{q_e} = \frac{1}{K_L Q_m} + \left(\frac{1}{Q_m}\right) C_e$	$Q_m$ (mg g <sup>-1</sup> )	73.47	82.94	120.59	390.53
		$K_L$ (L mg <sup>-1</sup> )	3.26	4.41	12.18	27.46
		$R_L$	0.057	0.043	0.016	0.007
		$R^2$	0.99	0.99	0.95	0.98
Freundlich	$\ln q_e = \ln K_F + \frac{1}{n} \ln C_e$	$n$	3.49	3.00	2.58	1.62
		$K_F$ (L mg <sup>-1</sup> )	23.35	21.58	20.99	22.63
		$R^2$	0.87	0.83	0.90	0.97
Temkin	$q_e = B_1 \ln k_i + B_1 \ln C_e$	$B_1$	12.35	15.27	20.95	30.84
		$k_i$ (L mg <sup>-1</sup> )	5.76	3.17	1.75	0.02
		$R^2$	0.91	0.92	0.89	0.96
Dubinin and Radushkevich	$\ln q_e = \ln Q_s - K\epsilon^2$	$Q_s$ (mg g <sup>-1</sup> )	64.64	73.24	81.74	206.3
		$K$	$5.65 \times 10^{-7}$	$1.3 \times 10^{-6}$	$8.28 \times 10^{-7}$	$2.33 \times 10^{-6}$
		$E$ (J mol <sup>-1</sup> ) = $1/(2K)^{1/2}$	940	620	776	462.7
		$R^2$	0.89	0.96	0.80	0.77

Table 9  
Comparison between the maximum adsorption capacity of DES treated MWACNTs and some reported adsorbents for 2,4-DCP removal

Adsorbent	$q_{max}$ (mg g <sup>-1</sup> )	REF
DES-S-MWCNTs	390.53	Present work
DES-P-MWCNTs	120.59	Present work
MWCNT	19.61	[31]
MWCNT-OH	20.9	[13]
MWCNTs-Fe <sub>3</sub> O <sub>4</sub> -Fe	7.1	[91]
CB-V carbon black	72.2	[92]
Carbonaceous adsorbent	277.7	[69]
Commercial AC (Prolabo)	256.4	[16]
AC from banana stalk	196.3	[93]
AC from apricot stone shells	339	[14]
AC from date stones	238.10	[89]
Coconut coir pith carbon	19.12	[94]
Palm pith carbon	19.16	[95]

isotherms under experimental conditions [73,87]. However, Langmuir isotherm yielded the better fit for all adsorbents with high R<sup>2</sup> value ranged from 0.95 to 0.99. This is an indication of a monolayer adsorption of 2,4-DCP onto the homogeneous surface of the used adsorbents. On the other hand, compared to the other adsorbents, the high R<sup>2</sup> value of Freundlich model for the two adsorbents of DES-P-MWCNTs and DES-S-MWCNTs suggests that different active sites with various affinities to 2,4-DCP molecules can lead the adsorption to take place onto the heterogeneous surface of these two adsorbents. Also, according to *n* value (>1) the adsorptive behavior is dominated as a physical adsorption process [88]. Furthermore, the value of  $R_L$  is found to be decreasing as the initial concentration of 2,4-DCP increases, proving again the applicability of Langmuir isotherm for the 2,4-DCP adsorption and the favorable adsorption of 2,4-DCP at higher initial concentration. A similar equilibrium results were obtained for the adsorption of 2,4-DCP onto AC derived from date stones [89] and onto AC derived from agricultural wastes [90]. Table 9 provides a comparison of the maximum monolayer adsorption capacity of 2,4-DCP on several adsorbents. As compared to previous works, in this study the MWCNTs adsorbent modified with sulfuric acid and DES (DES-S-MWCNTs) showed a remarkable value of maximum adsorption capacity of 390.35 mg g<sup>-1</sup>.

### 3.5. Mechanisms

The adsorption of 2,4-DCP onto the studied adsorbents was highly dependent on the characteristics of the adsorbent, the operational conditions, as well as on the molecular properties of 2,4-DCP. The oxygen-containing groups on functionalized MWCNTs played an important role in the adsorption of 2,4-DCP by enhancing the dispersion of MWCNTs in water. In addition, these groups defined the interaction between 2,4-DCP and the adsorbent surface through acting as acids or bases, which can adsorb 2,4-DCP through donor-acceptor complex formation. The molecu-

lar size of 2,4-DCP and its pKa value influenced its affinity towards MWCNTs surface. The interaction between the electron in the aromatic rings of 2,4-DCP and the graphene layer of MWCNTs may result into the  $\pi$ - $\pi$  phenomena which might involve charge-transfer, polar electrostatic components and dispersive forces [96]. Not to mention, controlling the pH value of the solution proved to have a remarkable impact on the adsorption mechanism. Since the phenolic compounds behave as weak acids in aqueous solution [97], the pH value of the solution has a strong effect on the dissociation of hydrogen ion from 2,4-DCP. The anionic form of 2,4-DCP is the predominant form when the value of solution pH is high, whereas the molecular form of 2,4-DCP dominates in acidic solutions [98]. In this study, for all cases of adsorbents, the optimum pH value which is required to obtain the highest removal efficiency was less than the pKa value of 2,4-DCP. Therefore, the mechanism of 2,4-DCP adsorption was mainly governed by the synergetic effects of  $\pi$ - $\pi$  interaction [99,100].

## 4. Conclusion

ChCl based DES was prepared using EG as HBD and applied as new functionalization agent for pristine MWCNTs and H<sub>2</sub>SO<sub>4</sub>-treated MWCNTs. RAMAN, FTIR, FESEM, BET, TEM, and TGA were used to study the changes occurred to MWCNTs after treatment with DES. It was concluded that DES purified and increased the surface area of MWCNTs, as well as added different functional groups on their surface conserving the structure of MWCNTs and without resulting in further damages. The efficiency of the DES-functionalized MWCNTs was investigated as new adsorbents for 2,4-DCP removal from water. Based on the optimization studies conducted by RSM-CCD experimental design, it was clear that the adsorption of 2,4-DCP was highly dependent on the pH solution, and on the surface charge of the adsorbents. The optimum pH value for all adsorbents was found to be less than pKa value of 2,4-DCP (>7.4). The 2,4-DCP adsorption kinetics for all examined adsorbents were well described by pseudo-second order model. The equilibrium adsorption data were best presented by Langmuir isotherm model indicating a monolayer adsorption on a homogeneous surface with the highest maximum adsorption capacity of 390.53 mg g<sup>-1</sup> obtained for MWCNTs functionalized with H<sub>2</sub>SO<sub>4</sub> and DES.

## Acknowledgement

The authors would like to express their gratitude to grant of the Geran Penyelidikan Universiti Malaya (UMRG Program) - AET (Innovative Technology (ITRC)), project number of RP019C-13AET, for the financial support.

## References

- [1] E. Bilgin Simsek, B. Aytas, D. Duranoglu, U. Beker, A.W. Trochimczuk, A comparative study of 2-chlorophenol, 2,4-dichlorophenol, and 2,4,6-trichlorophenol adsorption onto polymeric, commercial, and carbonaceous adsorbents, *Desal. Water Treat.*, 57 (2016) 9940–9956.

- [2] K. Kuśmierk, M. Szala, A. Świątkowski, Adsorption of 2,4-dichlorophenol and 2,4-dichlorophenoxyacetic acid from aqueous solutions on carbonaceous materials obtained by combustion synthesis, *J. Taiwan Inst. Chem. Eng.*, 63 (2016) 371–378.
- [3] C.-H. Lin, S.-K. Tseng, Electrochemically reductive dechlorination of pentachlorophenol using a high overpotential zinc cathode, *Chemosphere*, 39 (1999) 2375–2389.
- [4] Z. Jin, S.H. Zhang, X.G. Jian, Removal of 2, 4-dichlorophenol from wastewater by vacuum membrane distillation using hydrophobic PPESK hollow fiber membrane, *Chin. Chem. Lett.*, 18 (2007) 1543–1547.
- [5] S. Bhattacharya, R. Banerjee, Laccase mediated biodegradation of 2, 4-dichlorophenol using response surface methodology, *Chemosphere*, 73 (2008) 81–85.
- [6] M. Czaplicka, Sources and transformations of chlorophenols in the natural environment, *Sci. Total Environ.*, 322 (2004) 21–39.
- [7] E.O. Igbinosa, E.E. Odjajare, V.N. Chigor, I.H. Igbinosa, A.O. Emoghene, F.O. Ekhaie, N.O. Igiehon, O.G. Idemudia, Toxicological profile of chlorophenols and their derivatives in the environment: the public health perspective, *Sci. World J.*, 2013 (2013).
- [8] Q.-S. Liu, T. Zheng, P. Wang, J.-P. Jiang, N. Li, Adsorption isotherm, kinetic and mechanism studies of some substituted phenols on activated carbon fibers, *Chem. Eng. J.*, 157 (2010) 348–356.
- [9] N. Mubarak, J. Sahu, E. Abdullah, N. Jayakumar, P. Ganesan, Microwave assisted multiwall carbon nanotubes enhancing Cd (II) adsorption capacity in aqueous media, *J. Ind. Eng. Chem.*, 24 (2015) 24–33.
- [10] V.K. Gupta, A. Imran, Adsorbents for water treatment: development of low-cost alternatives to carbon, *Encycl. Surf. Colloid Sci.*, 2004 Update Supplement, 5 (2004) 1.
- [11] S.E. Bailey, T.J. Olin, R.M. Bricka, D.D. Adrian, A review of potentially low-cost sorbents for heavy metals, *Water Res.*, 33 (1999) 2469–2479.
- [12] H.M. Alayan, M.A. Alsaadi, R. Das, A. Abo-Hamad, R.K. Ibrahim, M.K. AlOmar, M.A. Hashim, The formation of hybrid carbon nanomaterial by chemical vapor deposition: an efficient adsorbent for enhanced adsorptive removal of methylene blue from aqueous solution, *Water Sci. Technol.*, (2018) wst2018211.
- [13] K. Kusmierk, M. Sankowska, A. Swiatkowski, Adsorption of dichlorophenols from aqueous solutions onto multi-walled carbon nanotubes, *Przem. Chem.*, 92 (2013) 1257–1260.
- [14] A.A.M. Daifullah, B.S. Girgis, Removal of some substituted phenols by activated carbon obtained from agricultural waste, *Water Res.*, 32 (1998) 1169–1177.
- [15] M.-W. Jung, K.-H. Ahn, Y. Lee, K.-P. Kim, J.-S. Rhee, J. Tae Park, K.-J. Paeng, Adsorption characteristics of phenol and chlorophenols on granular activated carbons (GAC), *Microchem. J.*, 70 (2001) 123–131.
- [16] O. Hamdaoui, E. Naffrechoux, Modeling of adsorption isotherms of phenol and chlorophenols onto granular activated carbon: Part I. Two-parameter models and equations allowing determination of the thermodynamic parameters, *J. Hazard. Mater.*, 147 (2007) 381–394.
- [17] X. Ren, C. Chen, M. Nagatsu, X. Wang, Carbon nanotubes as adsorbents in environmental pollution management: a review, *Chem. Eng. J.*, 170 (2011) 395–410.
- [18] R. Thines, N. Mubarak, S. Nizamuddin, J. Sahu, E. Abdullah, P. Ganesan, Application potential of carbon nanomaterials in water and wastewater treatment: A review, *J. Taiwan Inst. Chem. Eng.*, 72 (2017) 116–133.
- [19] N. Mubarak, J. Sahu, E. Abdullah, N. Jayakumar, Removal of heavy metals from wastewater using carbon nanotubes, *Sep. Purif. Rev.*, 43 (2014) 311–338.
- [20] N. Mubarak, J. Sahu, E. Abdullah, N. Jayakumar, P. Ganesan, Novel microwave-assisted multiwall carbon nanotubes enhancing Cu (II) adsorption capacity in water, *J. Taiwan Inst. Chem. Eng.*, 53 (2015) 140–152.
- [21] N.M. Mubarak, J.N. Sahu, E.C. Abdullah, N.S. Jayakumar, Rapid adsorption of toxic Pb(II) ions from aqueous solution using multiwall carbon nanotubes synthesized by microwave chemical vapor deposition technique, *J. Environ. Sci.*, 45 (2016) 143–155.
- [22] C. Chen, X. Wang, Adsorption of Ni (II) from aqueous solution using oxidized multiwall carbon nanotubes, *Ind. Eng. Chem. Res.*, 45 (2006) 9144–9149.
- [23] C. Luo, R. Wei, D. Guo, S. Zhang, S. Yan, Adsorption behavior of MnO<sub>2</sub> functionalized multi-walled carbon nanotubes for the removal of cadmium from aqueous solutions, *Chem. Eng. J.*, 225 (2013) 406–415.
- [24] M. Ruthiraan, N.M. Mubarak, R.K. Thines, E.C. Abdullah, J.N. Sahu, N.S. Jayakumar, P. Ganesan, Comparative kinetic study of functionalized carbon nanotubes and magnetic biochar for removal of Cd<sup>2+</sup> ions from wastewater, *Korean J. Chem. Eng.*, 32 (2015) 446–457.
- [25] R. Thines, N. Mubarak, M. Ruthiraan, E. Abdullah, J. Sahu, N. Jayakumar, P. Ganesan, N. Sajuni, Adsorption isotherm and thermodynamics studies of Zn (II) on functionalized and non-functionalized carbon nanotubes, *Adv. Sci., Eng. Med.*, 6 (2014) 974–984.
- [26] M.H. Dehghani, M. Mostofi, M. Alimohammadi, G. McKay, K. Yetilmezsoy, A.B. Albadarin, B. Heibati, M. AlGhouti, N.M. Mubarak, J.N. Sahu, High-performance removal of toxic phenol by single-walled and multi-walled carbon nanotubes: Kinetics, adsorption, mechanism and optimization studies, *J. Ind. Eng. Chem.*, 35 (2016) 63–74.
- [27] X. Peng, Y. Li, Z. Luan, Z. Di, H. Wang, B. Tian, Z. Jia, Adsorption of 1, 2-dichlorobenzene from water to carbon nanotubes, *Chem. Phys. Lett.*, 376 (2003) 154–158.
- [28] G.-C. Chen, X.-Q. Shan, Y.-S. Wang, B. Wen, Z.-G. Pei, Y.-N. Xie, T. Liu, J.J. Pignatello, Adsorption of 2,4,6-trichlorophenol by multi-walled carbon nanotubes as affected by Cu(II), *Water Res.*, 43 (2009) 2409–2418.
- [29] M. Abdel Salam, R.C. Burk, Thermodynamics of pentachlorophenol adsorption from aqueous solutions by oxidized multi-walled carbon nanotubes, *Appl. Surf. Sci.*, 255 (2008) 1975–1981.
- [30] C.-H. Wu, Adsorption of reactive dye onto carbon nanotubes: equilibrium, kinetics and thermodynamics, *J. Hazard. Mater.*, 144 (2007) 93–100.
- [31] J. Xu, X. Lv, J. Li, Y. Li, L. Shen, H. Zhou, X. Xu, Simultaneous adsorption and dechlorination of 2,4-dichlorophenol by Pd/Fe nanoparticles with multi-walled carbon nanotube support, *J. Hazard. Mater.*, 225–226 (2012) 36–45.
- [32] M.M. Aljumaily, M.A. Alsaadi, R. Das, S.B.A. Hamid, N.A. Hashim, M.K. AlOmar, H.M. Alayan, M. Novikov, Q.F. Alsally, M.A. Hashim, Optimization of the synthesis of superhydrophobic carbon nanomaterials by chemical vapor deposition, *Sci. Rep.*, 8 (2018) 2778.
- [33] R.K. Ibrahim, M. Hayyan, M.A. AlSaadi, A. Hayyan, S. Ibrahim, Environmental application of nanotechnology: air, soil, and water, *Environ. Sci. Pollut. Res.*, (2016) 1–35.
- [34] B. Yu, F. Zhou, G. Liu, Y. Liang, W.T. Huck, W. Liu, The electrolyte switchable solubility of multi-walled carbon nanotube/ionic liquid (MWCNT/IL) hybrids, *Chem. Commun.*, (2006) 2356–2358.
- [35] A. Pénicaud, P. Poulin, A. Derré, E. Anglaret, P. Petit, Spontaneous dissolution of a single-wall carbon nanotube salt, *J. Am. Chem. Soc.*, 127 (2005) 8–9.
- [36] V. Datsyuk, M. Kalyva, K. Papagelis, J. Parthenios, D. Tasis, A. Siokou, I. Kallitsis, C. Galiotis, Chemical oxidation of multi-walled carbon nanotubes, *Carbon*, 46 (2008) 833–840.
- [37] N.M. Mubarak, R.F. Alicia, E.C. Abdullah, J.N. Sahu, A.B.A. Haslija, J. Tan, Statistical optimization and kinetic studies on removal of Zn<sup>2+</sup> using functionalized carbon nanotubes and magnetic biochar, *J. Environ. Chem. Eng.*, 1 (2013) 486–495.
- [38] E. Durand, J. Lecomte, P. Villeneuve, Deep eutectic solvents: Synthesis, application, and focus on lipase-catalyzed reactions, *Eur. J. Lipid Sci. Technol.*, 115 (2013) 379–385.
- [39] B. Tang, K. Row, Recent developments in deep eutectic solvents in chemical sciences, *Monatsh Chem*, 144 (2013) 1427–1454.
- [40] Y.R. Lee, K.H. Row, Comparison of ionic liquids and deep eutectic solvents as additives for the ultrasonic extraction of astaxanthin from marine plants, *Ind. Eng. Chem.*
- [41] A. Abo-Hamad, M. Hayyan, M.A. AlSaadi, M.A. Hashim, Potential applications of deep eutectic solvents in nanotechnology, *Chem. Eng. J.*, 273 (2015) 551–567.

- [42] P.D. de María, Z. Maugeri, Ionic liquids in biotransformations: from proof-of-concept to emerging deep-eutectic-solvents, *Curr. Opin. Chem. Biol.*, 15 (2011) 220–225.
- [43] R.K. Ibrahim, M. Hayyan, M.A. Alsaadi, S. Ibrahim, A. Hayyan, M.A. Hashim, Diethylene glycol based deep eutectic solvents and their physical properties, *Stud. Univ. Babeş-Bolyai, Chem.*, 62 (2017).
- [44] V.S. Raghuvanshi, M. Ochmann, A. Hoell, F. Polzer, K. Rademann, Deep eutectic solvents for the self-assembly of gold nanoparticles: A SAXS, UV-Vis, and TEM investigation, *Langmuir*, 30 (2014) 6038–6046.
- [45] C. Gu, Y. Mai, J. Zhou, J. Tu, SnO<sub>2</sub> nanocrystallite: novel synthetic route from deep eutectic solvent and lithium storage performance, *Funct. Mater. Lett.*, 4 (2011) 377–381.
- [46] M. Hayyan, A. Abo-Hamad, M.A. AlSaadi, M.A. Hashim, Functionalization of graphene using deep eutectic solvents, *Nanoscale Res. Lett.*, 10 (2015) 1.
- [47] M.K. AlOmar, M.A. Alsaadi, M. Hayyan, S. Akib, M.A. Hashim, Functionalization of CNTs surface with phosphonium based deep eutectic solvents for arsenic removal from water, *Appl. Surf. Sci.*, 389 (2016) 216–226.
- [48] M.K. AlOmar, M.A. Alsaadi, M. Hayyan, S. Akib, M. Ibrahim, M.A. Hashim, Allyl triphenyl phosphonium bromide based DES-functionalized carbon nanotubes for the removal of mercury from water, *Chemosphere*, 167 (2017) 44–52.
- [49] M.K. AlOmar, M.A. Alsaadi, M. Hayyan, S. Akib, R.K. Ibrahim, M.A. Hashim, Lead removal from water by choline chloride based deep eutectic solvents functionalized carbon nanotubes, *J. Mol. Liq.*, (2016).
- [50] A. Ferrari, J. Meyer, V. Scardaci, C. Casiraghi, M. Lazzeri, F. Mauri, S. Piscanec, D. Jiang, K. Novoselov, S. Roth, Raman spectrum of graphene and graphene layers, *Phys. Rev. Lett.*, 97 (2006) 187401.
- [51] Y. Ying, R.K. Saini, F. Liang, A.K. Sadana, W. Billups, Functionalization of carbon nanotubes by free radicals, *Org. Lett.*, 5 (2003) 1471–1473.
- [52] J.L. Bahr, J. Yang, D.V. Kosynkin, M.J. Bronikowski, R.E. Smalley, J.M. Tour, Functionalization of carbon nanotubes by electrochemical reduction of aryl diazonium salts: A bucky paper electrode, *J. Am. Chem. Soc.*, 123 (2001) 6536–6542.
- [53] M.S. Dresselhaus, A. Jorio, M. Hofmann, G. Dresselhaus, R. Saito, Perspectives on carbon nanotubes and graphene Raman spectroscopy, *Nanoletters*, 10 (2010) 751–758.
- [54] A. Jorio, M. Pimenta, A. Souza Filho, R. Saito, G. Dresselhaus, M. Dresselhaus, Characterizing carbon nanotube samples with resonance Raman scattering, *New J. Phys.*, 5 (2003) 139.
- [55] C. Tsai, C. Chen, Characterization of bias-controlled carbon nanotubes, *Diamond Relat. Mater.*, 12 (2003) 1615–1620.
- [56] C. Lu, H. Bai, B. Wu, F. Su, J.F. Hwang, Comparative study of CO<sub>2</sub> capture by carbon nanotubes, activated carbons, and zeolites, *Energy Fuels*, 22 (2008) 3050–3056.
- [57] J. Coates, Interpretation of infrared spectra, a practical approach, in: *Encyclopedia of Analytical Chemistry*, 2000.
- [58] A.K. Das, S. Maiti, B. Khatua, High performance electrode material prepared through in-situ polymerization of aniline in the presence of zinc acetate and graphene nanoplatelets for supercapacitor application, *J. Electroanal. Chem.*, 739 (2015) 10–19.
- [59] F.M. Machado, C.P. Bergmann, T.H. Fernandes, E.C. Lima, B. Royer, T. Calvete, S.B. Fagan, Adsorption of Reactive Red M-2BE dye from water solutions by multi-walled carbon nanotubes and activated carbon, *J. Hazard. Mater.*, 192 (2011) 1122–1131.
- [60] S. Maiti, B.B. Khatua, Electrochemical and electrical performances of cobalt chloride (CoCl<sub>2</sub>) doped polyaniline (PANI)/graphene nanoplate (GNP) composite, *RSC Adv.*, 3 (2013) 12874–12885.
- [61] G.D. Sheng, D.D. Shao, X.M. Ren, X.Q. Wang, J.X. Li, Y.X. Chen, X.K. Wang, Kinetics and thermodynamics of adsorption of ionizable aromatic compounds from aqueous solutions by as-prepared and oxidized multiwalled carbon nanotubes, *J. Hazard. Mater.*, 178 (2010) 505–516.
- [62] B.H. Stuart, *Infrared Spectroscopy: Fundamentals and Applications*/H. Barbara Stuart, in: Wiley, 2004, 224 p.
- [63] P. Hou, C. Liu, Y. Tong, S. Xu, M. Liu, H. Cheng, Purification of single-walled carbon nanotubes synthesized by the hydrogen arc-discharge method, *J. Mater. Res.*, 16 (2001) 2526–2529.
- [64] A. Rinzler, J. Liu, H. Dai, P. Nikolaev, C. Huffman, F. Rodriguez-Macias, P. Boul, A. Lu, D. Heymann, D. Colbert, Large-scale purification of single-wall carbon nanotubes: process, product, and characterization, *Appl. Phys. A: Mater. Sci. Process.*, 67 (1998) 29–37.
- [65] P. Ajayan, T. Ebbesen, T. Ichihashi, S. Iijima, K. Tanigaki, H. Hiura, Opening carbon nanotubes with oxygen and implications for filling, *Nature*, 362 (1993) 522–525.
- [66] C. Lu, H. Chiu, Chemical modification of multiwalled carbon nanotubes for sorption of Zn<sup>2+</sup> from aqueous solution, *Chem. Eng. J.*, 139 (2008) 462–468.
- [67] J. Fan, Z. Shi, M. Tian, J. Wang, J. Yin, Unzipped multiwalled carbon nanotube oxide/multiwalled carbon nanotube hybrids for polymer reinforcement, *ACS Appl. Mater. Interfaces*, 4 (2012) 5956–5965.
- [68] O.V. Kharissova, B.I. Kharisov, E.G. de Casas Ortiz, Dispersion of carbon nanotubes in water and non-aqueous solvents, *RSC Adv.*, 3 (2013) 24812–24852.
- [69] V.K. Gupta, I. Ali, V.K. Saini, Adsorption of 2, 4-D and carbofuran pesticides using fertilizer and steel industry wastes, *J. Colloid Interface Sci.*, 299 (2006) 556–563.
- [70] J.-W. Ma, H. Wang, F.-Y. Wang, Z.-H. Huang, Adsorption of 2, 4-dichlorophenol from aqueous solution by a new low-cost adsorbent-activated bamboo charcoal, *Sep. Sci. Technol.*, 45 (2010) 2329–2336.
- [71] R. Darvishi Cheshmeh Soltani, A. Khataee, H. Godini, M. Safari, M. Ghanadzadeh, M. Rajaei, Response surface methodological evaluation of the adsorption of textile dye onto biosilica/alginate nanobiocomposite: thermodynamic, kinetic, and isotherm studies, *Desal. Water Treat.*, 56 (2015) 1389–1402.
- [72] S. Lagergren, *About the Theory of So-Called Adsorption of Soluble Substances*, 1898.
- [73] D.K. Mahmoud, M.A.M. Salleh, W.A.W.A. Karim, A. Idris, Z.Z. Abidin, Batch adsorption of basic dye using acid treated kenaf fibre char: equilibrium, kinetic and thermodynamic studies, *Chem. Eng. J.*, 181 (2012) 449–457.
- [74] S. Lagergren, *Zur theorie der sogenannten adsorption gelöster stoffe*. Kungliga Svenska Vetenskapsakademiens, *Handlingar*, 24 (1898) 1–39.
- [75] F.W. Shaarani, B.H. Hameed, Ammonia-modified activated carbon for the adsorption of 2,4-dichlorophenol, *Chem. Eng. J.*, 169 (2011) 180–185.
- [76] Y.-S. Ho, G. McKay, Sorption of dye from aqueous solution by peat, *Chem. Eng. J.*, 70 (1998) 115–124.
- [77] J.-P. Wang, H.-M. Feng, H.-Q. Yu, Analysis of adsorption characteristics of 2, 4-dichlorophenol from aqueous solutions by activated carbon fiber, *J. Hazard. Mater.*, 144 (2007) 200–207.
- [78] L. Wang, J. Zhang, R. Zhao, C. Zhang, C. Li, Y. Li, Adsorption of 2,4-dichlorophenol on Mn-modified activated carbon prepared from *Polygonum orientale* Linn, *Desalination*, 266 (2011) 175–181.
- [79] F.A. Pavan, S.L. Dias, E.C. Lima, E.V. Benvenuti, Removal of Congo red from aqueous solution by anilinepropylsilica xerogel, *Dyes Pigm.*, 76 (2008) 64–69.
- [80] V. Vimonse, S. Lei, B. Jin, C.W. Chow, C. Saint, Kinetic study and equilibrium isotherm analysis of Congo Red adsorption by clay materials, *Chem. Eng. J.*, 148 (2009) 354–364.
- [81] Y.-S. Ho, G. McKay, Pseudo-second order model for sorption processes, *Process Biochem.*, 34 (1999) 451–465.
- [82] G. McKay, M. El Geundi, M. Nassar, Equilibrium studies during the removal of dyestuffs from aqueous solutions using bagasse pith, *Water Res.*, 21 (1987) 1513–1520.
- [83] Z. Zhang, Z. Zhang, Y. Fernández, J. Menéndez, H. Niu, J. Peng, L. Zhang, S. Guo, Adsorption isotherms and kinetics of methylene blue on a low-cost adsorbent recovered from a spent catalyst of vinyl acetate synthesis, *Appl. Surf. Sci.*, 256 (2010) 2569–2576.
- [84] K. Hall, L. Eagleton, A. Acrivos, T. Vermeulen, Pore-and solid-diffusion kinetics in fixed-bed adsorption under constant-pattern conditions, *Ind. Eng. Chem. Fundam.*, 5 (1966) 212–223.

- [85] F. Haghseresht, G. Lu, Adsorption characteristics of phenolic compounds onto coal-reject-derived adsorbents, *Energy Fuels*, 12 (1998) 1100–1107.
- [86] B.H. Hameed, A.A. Ahmad, N. Aziz, Isotherms, kinetics and thermodynamics of acid dye adsorption on activated palm ash, *Chem. Eng. J.*, 133 (2007) 195–203.
- [87] C. Namasivayam, R. Jeyakumar, R. Yamuna, Dye removal from wastewater by adsorption on 'waste'Fe (III)/Cr (III) hydroxide, *Waste Manage.*, 14 (1994) 643–648.
- [88] A.S. Özcan, B. Erdem, A. Özcan, Adsorption of Acid Blue 193 from aqueous solutions onto BTMA-bentonite, *Colloids Surf., A*, 266 (2005) 73–81.
- [89] B. Hameed, J. Salman, A. Ahmad, Adsorption isotherm and kinetic modeling of 2, 4-D pesticide on activated carbon derived from date stones, *J. Hazard. Mater.*, 163 (2009) 121–126.
- [90] F. Shaarani, B. Hameed, Batch adsorption of 2, 4-dichlorophenol onto activated carbon derived from agricultural waste, *Desalination*, 255 (2010) 159–164.
- [91] J. Xu, X. Liu, G.V. Lowry, Z. Cao, H. Zhao, J.L. Zhou, X. Xu, Dechlorination mechanism of 2, 4-dichlorophenol by magnetic MWCNTs supported Pd/Fe nanohybrids: rapid adsorption, gradual dechlorination, and desorption of phenol, *ACS Appl. Mater. Interf.*, 8 (2016) 7333–7342.
- [92] K. Kuśmierk, M. Szala, A. Świątkowski, Adsorption of 2, 4-dichlorophenol and 2, 4-dichlorophenoxyacetic acid from aqueous solutions on carbonaceous materials obtained by combustion synthesis, *J. Taiwan Inst. Chem. Eng.*, 63 (2016) 371–378.
- [93] J. Salman, V. Njoku, B. Hameed, Adsorption of pesticides from aqueous solution onto banana stalk activated carbon, *Chem. Eng. J.*, 174 (2011) 41–48.
- [94] C. Namasivayam, D. Kavitha, Adsorptive removal of 2, 4-dichlorophenol from aqueous solution by low-cost carbon from an agricultural solid waste: coconut coir pith, *Separ. Sci. Technol.*, 39 (2005) 1407–1425.
- [95] M. Sathishkumar, A. Binupriya, D. Kavitha, S. Yun, Kinetic and isothermal studies on liquid-phase adsorption of 2, 4-dichlorophenol by palm pith carbon, *Bioresour. Technol.*, 98 (2007) 866–873.
- [96] M.-W. Jung, K.-H. Ahn, Y. Lee, K.-P. Kim, J.-S. Rhee, J.T. Park, K.-J. Paeng, Adsorption characteristics of phenol and chlorophenols on granular activated carbons (GAC), *Microchem. J.*, 70 (2001) 123–131.
- [97] A. Demirak, Ö. Dalman, E. Tilkan, D. Yıldız, E. Yavuz, C. Gökçe, Biosorption of 2, 4 dichlorophenol (2, 4-DCP) onto *Posidonia oceanica* (L.) seagrass in a batch system: Equilibrium and kinetic modeling, *Microchem. J.*, 99 (2011) 97–102.
- [98] S.K. Nadavala, K. Swayampakula, V.M. Boddu, K. Abburi, Biosorption of phenol and o-chlorophenol from aqueous solutions on to chitosan-calcium alginate blended beads, *J. Hazard. Mater.*, 162 (2009) 482–489.
- [99] J.-P. Wang, Y.-Z. Chen, H.-M. Feng, S.-J. Zhang, H.-Q. Yu, Removal of 2, 4-dichlorophenol from aqueous solution by static-air-activated carbon fibers, *J. Colloid Interface Sci.*, 313 (2007) 80–85.
- [100] E. Luboch, E. Wagner-Wysiecka, Z. Poleska-Muchlado, V.C. Kravtsov, Synthesis and properties of azobenzocrown ethers with  $\pi$ -electron donor, or  $\pi$ -electron donor and  $\pi$ -electron acceptor group (s) on benzene ring (s), *Tetrahedron*, 61 (2005) 10738–10747.

## Supporting information

Table S1

List of design of experiments runs and the actual values obtained from each response for all adsorbents

Run	Factors			Response of P-MWCNTs		Response of S-MWCNTs		Response of DES-P-MWCNTs		Response of DES-S-MWCNTs	
	A	B	C	Removal %	Adsorption capacity (mg/g)	Removal %	Adsorption capacity (mg/g)	Removal %	Adsorption capacity (mg/g)	Removal %	Adsorption capacity (mg/g)
1	2	5	20	29.357	32	38.532	42	28.440	31	39.449	43
2	6	15	40	80.612	26.333	75.510	24.6667	69.387	22.67	76.530	25
3	2	5	60	37.614	41	44.036	48	37.614	41	37.614	41
4	10	5	20	1.8518	3	-9.629	-13	-0.617	-1	8.0246	13
5	10	10	40	19.135	15.5	15.555	10.5	19.135	15.5	30.246	24.5
6	10	15	20	5.555	3	-7.407	-3.333	1.851	1	9.259	5
7	2	15	60	77.981	28.33	67.889	24.6667	71.559	26	52.293	19
8	6	10	40	67.346	33	66.326	32.5	63.265	31	69.387	34
9	10	15	60	-4.761	-2.333	-5.185	-2.333	-8.843	-4.333	0.680	0.333
10	6	10	60	62.244	30.5	57.142	28	47.959	23.5	55.102	27
11	6	10	20	64.285	31.5	66.326	32.5	61.224	30	61.224	30
12	10	5	60	4.320	7	3.703	5	3.086	5	21.604	35
13	2	15	20	74.311	27	66.972	24.33	64.220	23.33	61.467	22.33

A: pH, B: adsorbent dosage and C: contact time

Table S2

Reduced cubic model analysis of variance (ANOVA) for 2,4-DCP removal (%) by P-MWCNTs and S-MWCNTs

Source*	P-MWCNTs					S-MWCNTs				
	Sum of squares	df	Mean square	F-value	p-value prob > F	Sum of squares	df	Mean square	F-value	p-value prob > F
Model	12522.18	9	1391.35	80.02	0.0021	12863.17	9	1429.24	29.69	0.0089
A	5608.55	1	5608.55	322.58	0.0004	6922.20	1	6922.20	143.80	0.0012
B	863.48	1	863.48	49.66	0.0059	298.26	1	298.26	6.20	0.0886
C	0.42	1	0.42	0.024	0.8870	16.37	1	16.37	0.34	0.6008
AB	1028.32	1	1028.32	59.14	0.0046	434.54	1	434.54	9.03	0.0575
AC	48.88	1	48.88	2.81	0.1922	10.43	1	10.43	0.22	0.6733
BC	37.73	1	37.73	2.17	0.2371	30.80	1	30.80	0.64	0.4822
A <sup>2</sup>	1211.23	1	1211.23	69.66	0.0036	1272.92	1	1272.92	26.44	0.0143
B <sup>2</sup>	25.83	1	25.83	1.49	0.3100	38.23	1	38.23	0.79	0.4385
C <sup>2</sup>	173.06	1	173.06	9.95	0.0511	224.89	1	224.89	4.67	0.1194
	<b>Adj R-Squared**</b>		<b>0.98</b>	<b>Pred R-Squared</b>	<b>0.91</b>	<b>Adj R-Squared**</b>		<b>0.95</b>	<b>Pred R-Squared</b>	<b>0.82</b>
	<b>C.V. %</b>		<b>10.43</b>	<b>Std. Dev</b>	<b>4.17</b>	<b>C.V. %</b>		<b>18.80</b>	<b>Std. Dev</b>	<b>6.94</b>

\*A: pH, B: adsorbent dosage and C: contact time; \*\* The "Pred R-Squared" is in reasonable agreement with the "Adj R-Squared".

Table S3

List of the actual and predicted values for 2,4-DCP removal % response

Run order	P-MWCNTs		S-MWCNTs		DES-P-MWCNTs		DES-S-MWCNTs	
	Actual value	Predicted value						
1	29.36	28.34	38.53	38.84	28.44	28.25	39.45	37.8
2	1.85	3.48	-9.63	-7	-0.62	2.7	8.02	10.6
3	74.31	75.94	66.97	69.6	64.22	67.54	61.47	64.04
4	5.56	5.74	-7.41	-5.71	1.85	2.4	9.26	8.64
5	37.61	38.03	44.04	43.04	37.61	37.44	37.61	38.75
6	4.32	3.29	3.7	1.77	3.09	0.14	21.6	19.55
7	77.98	76.95	67.89	65.95	71.56	68.61	52.29	50.24
8	-4.76	-3.14	-5.19	-4.8	-8.84	-8.28	0.68	2.84
9	19.14	16.72	15.56	12.78	19.14	17.65	30.25	28.19
10	67.35	72.17	66.33	71.88	63.27	66.23	69.39	73.5
11	80.61	78.2	75.51	72.74	69.39	67.91	76.53	74.47
12	64.29	61.86	66.33	59.07	61.22	54.23	61.22	58.35
13	62.24	62.26	57.14	61.63	47.96	53.48	55.1	55.92

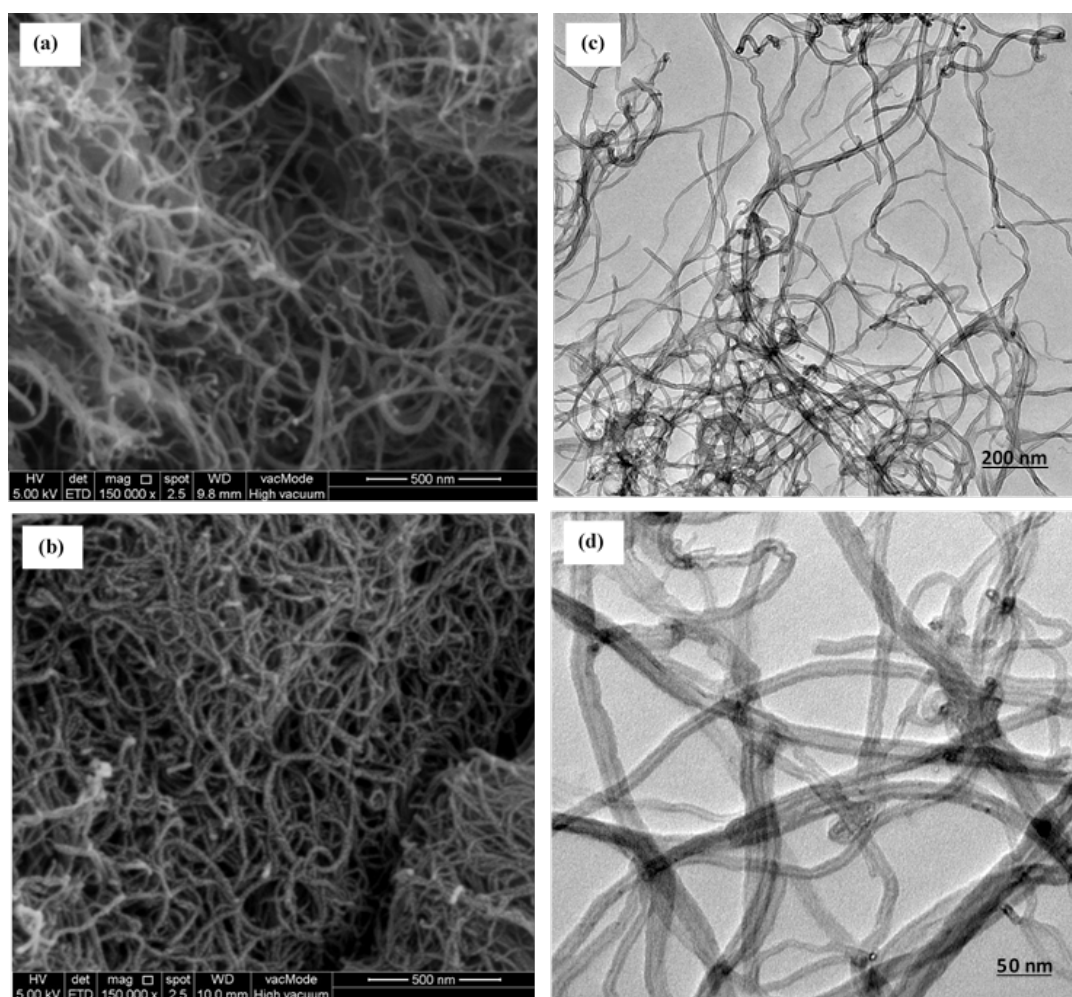


Fig. S1. FESEM images for a) S-MWCNTs, b) DES-P-MWCNTs; and TEM images for c) S-MWCNTs, d) DES-P-MWCNTs

Table S4  
Optimum adsorption conditions suggested by DOE software for all adsorbents

Adsorbent	pH	Dose (mg/g)	Contact time (min)	Predicted removal (%)	Predicted adsorption capacity (mg/g)	Desirability
P-MWCNTs	4.11	9.68	41.65	77.0919	40.9999	0.887
S-MWCNTs	3.97	8.23	41.56	74.8842	44.774	0.933
DES-P-MWCNTs	3.69	9.35	41.42	71.5545	41.0002	0.922
DES-S-MWCNTs	5.14	5.00	41.25	71.0324	43.3178	0.948

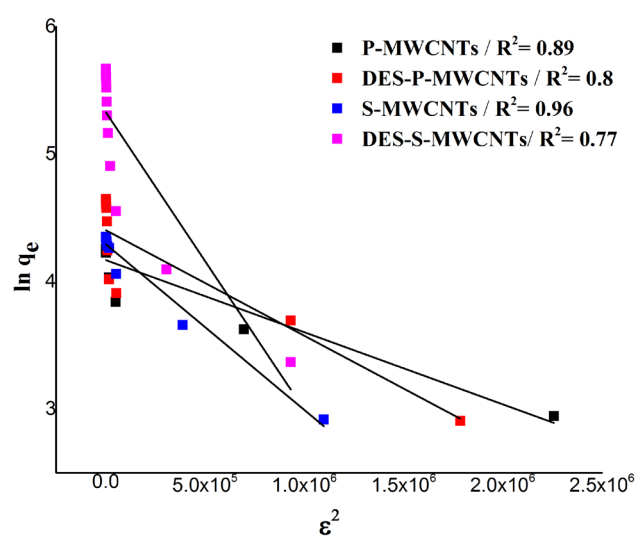


Fig. S2. Dubinin–Radushkevich isotherm model plot of 2,4-DCP sorption on P-MWCNTs, S-MWCNTs, DES-P-MWCNTs, and DES-S-MWCNTs surface at optimum pH of each adsorbent.